Steel and Composite Structures, *Vol. 29, No. 3 (2018) 349-362*
DOI: https://doi.org/10.12989/scs.2018.29.3.349

Thermal buckling of smart porous functionally graded nanobeam rested on Kerr foundation

Behrouz Karami [*1], Davood Shahsavari [1],
Seyed Mohammad Reza Nazemosadat [2,3], Li Li [**4] and Arash Ebrahimi [5]

[1] *Department of Mechanical Engineering, Marvdasht Branch, Islamic Azad University, Marvdasht, Iran*
[2] *Sama Technical and Vocational Training College, Islamic Azad University, Shiraz Branch, Shiraz, Iran*
[3] *Department of Mechanical Engineering of Biosystems, Shahrekord University, Shahrekord, Iran*
[4] *State Key Lab of Digital Manufacturing Equipment and Technology, School of Mechanical Science and Engineering, Huazhong University of Science and Technology, Wuhan 430074, China*
[5] *Faculty of Computer Science and Electrical Engineering, University of Rostock, Albert-Einstein-Straße 2, Rostock 18059, Germany*

(*Received April 3, 2018, Revised August 14, 2018, Accepted September 25, 2018*)

Abstract. Thermal buckling behavior of porous functionally graded nanobeam integrated with piezoelectric sensor and actuator based on the nonlocal higher-order shear deformation beam theory is investigated for the first time. Its material properties are assumed to be temperature-dependent and varying along the thickness direction according to the modified power-law rule. Note that the porosity with even type is considered herein. The equations of motion are obtained through Hamilton's principle. The influences of several parameters (such as type of temperature distribution, external electric voltage, material composition, porosity, small-scale effect, Ker foundation parameters, and beam thickness) on the thermal buckling of FG nanobeam are investigated in detail.

Keywords: thermal buckling; higher-order shear deformation beam theory; functionally graded nanobeam; nonlocal elasticity theory; Kerr elastic foundation

1. Introduction

Due to the mixture of elements (ceramic and metal) along the thickness direction, there are multiple benefits for using functionally graded materials (FGMs) in advanced engineering structures. Because at the same time, the metal element provides a reliable mechanical performance in the structural system for decreasing the probability of fracture while the ceramic element gives the high thermal resistance inside these materials (Karami *et al*. 2018a, b, f, j, She *et al*. 2018d, Yang and Yu 2017). Moreover, combination of piezoelectric layers has engineering innovations for controlling vibration, stability, and deformation acoustics of FGMs. (Rouzegar and Abad 2015) showed that, the increment in thickness of piezoelectric layers leads to higher mass density and lower elastic moduli of FG plate, and takes higher natural frequencies. An analytical solution was presented for the nonlinear post-buckling analysis of functionally graded carbon nanotubes reinforced composite (FG-CNTRC) cylindrical shells with piezoelectric layers by (Ansari *et al*. 2016). Damped free vibration of same materials bounded with piezoelectric sensor and actuator layers are studied by (Ghorbanpour Arani *et al*. 2017).

On the other hand, it is known that during fabrication process of FGMs and in the sintering step, due to the gap between solidification temperatures of elements, different patterns of voids or porosities can be generated (Li *et al*. 2003, Zhu *et al*. 2001). Therefore, considering and modeling of the behavior of FGMs with porosities can be applicable and important for their optimal design. In order to appropriate predict of FGM with porosities, several numerical and analytical models have been proposed for beam/plate type structures including porosity in recent years. Linear and nonlinear vibration characteristics of imperfect FG beams with porosities were studied by (Wattanasakulpong and Ungbhakorn 2014). In this work, even and uneven porosity distributions were considered using a modified power-law index. The wave propagation of FG plates including even porosities with application in ultrasonic inspection techniques was examined by (Yahia *et al*. 2015). Buckling and static bending analysis of FG beam porous were presented by (Chen *et al*. 2015). Gupta and Talha (2017) analyzed the influence of porosity on the vibration behavior of FG plates in the presence of thermal environment by applying a non-polynomial higher-order shear and normal deformation theory. They showed, with increment in the temperature difference between the two elements (ceramic and metal), the frequency will be decreased. A refined-trigonometric shear deformation theory (R-TSDT) was applied for the thermo/elastic bending response of FG sandwich plates by (Tounsi *et al*. 2013). Again, it was indicated that the temperature

∗Corresponding author, Ph.D. Student,
E-mail: behrouz.karami@miau.ac.ir

∗∗Co-corresponding author, Ph.D.,
E-mail: lili_em@hust.edu.cn

http://www.techno-press.org/?journal=scs&subpage=6
ISSN: 1229-9367 (Print), 1598-6233 (Online)

possesses considerable role on determining the behaviors of porous FG plates.

With the rapid development of using nanoscale structures in engineering applications due to their benefits, FGMs with porosities have gained interest among researchers. Furthermore, at micro/nano-scale, it has been proved that the mechanical behaviors of structures possess size dependency via some experimental studies. Hence, it is requisite to predicting the size-dependent specifications of structures in this scale. Consequently, wide ranges of non-classical continuum elasticity theories have been introduced to capture the size-dependent effects when the scale of structures tend to micro/nano scale (Karami and Janghorban 2016, Karami *et al*. 2017, Karami *et al*. 2018c, d, f, j, Shahsavari *et al*. 2018a, b, She *et al*. 2018a, e, 2017b, c). Among non-classical continuum theories for thinking the size-dependent effects, the nonlocal elasticity theory. Eringen (1983) offered by Eringen is an ideal model for comparison with the old ones (classical continuum theories) which didn't consider the size-dependent effects. On the basis of this theory, the size-dependent effect counts with only one small-scale parameter (known as the nonlocal parameter). Based on this theory, the strain-driven nonlocal elastic theory characterizes that the stress field at a reference point in an elastic continuum depends not only on strain at that point, but also on strains at all other points in the domain of interest (Lim *et al*. 2010, Wang and Duan 2008, Yang *et al*. 2010). The strain-driven nonlocal integral model is difficult to solve. Since the strain-driven nonlocal integral model equipped with Helmholtz averaging kernel can be equivalently transformed as a nonlocal differential model for unbounded domain problems, as shown by Eringen in his original paper (Eringen 1983). The nonlocal differential model may be called Eringen Nonlocal Differential Model (ENDM). In spite of the limitations of ENDM in some cases (Romano *et al*. 2017a, 2018), due to the fact that the ENDM can be easily addressed and it has been proved to show good agreement with molecular dynamic results (Hu *et al*. 2008, Wang and Hu 2008), it has been widely chosen in many works for investigating on the behaviors of numerous nanoscale structures (Karami et al. 2018e, g, Shahsavari and Janghorban 2017, Shahsavari *et al*. 2017b). Thermal buckling analysis of FG nanosize plates based on trigonometric shear deformation theory is conducted by (Khetir *et al*. 2017). Based on Timoshenko beam theory, (Ebrahimi and Daman 2017) examined dynamic behavior of curved inhomogeneous structures with porosities exposed to thermal environment. Application of nonlocal elasticity theory in Hygro-thermo-mechanical vibration and buckling analysis of exponentially graded nanoplates resting on elastic foundation is investigated by (Sobhy 2017) based on four-unknown shear deformation plate theory. For porous beam and plates in nano scale, several models were proposed so far (Karami et al. 2018e; She *et al*. 2018b, c). Free vibration of imperfect FG nanoplates with porosities using nonlocal elasticity theory and also Monte Carlo method was examined by Mechab *et al*. (2016b). Matching results between the nonlocal elasticity theory and also Monte Carlo method showed the importance of porosity in the formulation in order to obtain accurate results. Nonlocal elasticity theory in connection with third-order shear deformation plate theory was developed in order to examine the size-dependent free vibration analysis of porosity-dependent magneto-electro-elastic functionally graded (MEE-FG) nanobeams by (Ebrahimi and Barati 2017). The even and uneven porosity distribution was used for nonlinear vibration analysis of FG nanobeam on the basis of a size-dependent Euler–Bernoulli beam model by (Li *et al*. 2018). Size-dependent nonlinear buckling analysis of FG nanobeams including porosity was examined using nonlocal elasticity theory and generalized differential quadrature method by Shafiei and Kazemi (2017). Mechab *et al*. (2016a) analyzed the frequency of nanoplates made of FGM rested on Winkler-Pasternak elastic foundation using nonlocal elasticity theory and two-variable refined plate theory. Guided wave propagation in fully clamped FG nanoporous plates rested on Winkler-Pasternak foundation via nonlocal first deformation theory were investigated by (Karami *et al*. 2018e) for the first time. Recently, (Karami *et al*. 2018f) studied the wave analysis of temperature-dependent FG nanoplates with even porosity patterns based on a nonlocal strain gradient second shear deformation theory. They showed that the porous materials are very sensitive to the variation of environment temperature.

When identically acknowledged that by adding constitutive boundary conditions in strain-driven nonlocal integral models, the problems caused by the equilibrium and constitutive conditions in the stress field become improper (Barretta *et al*. 2018a, b, Romano and Barretta 2017, Romano *et al*. 2017a, b). Hence, a right solution of strain-driven nonlocal integral models may not exist (Barretta *et al*. 2016, Challamel and Wang 2008, Li *et al*. 2015). This caused to report of the results of contradictions inside some works (Barretta *et al*. 2016, Li *et al*. 2015, Zhu and Li 2017b). This crucial problem can be defeated by performing a stress-driven nonlocal integral model according to the suggestion in Romano and Barretta (2017) where the impact of stress and elastic strain fields are swapped.

The critical buckling, material stiffness and also fracture toughness of structures will be further surveyed by incorporation of an elastic foundation in the system. Among elastic foundations, the Winkler model with incorporation a linear series of springs has most cited and used in the literature due to its simplicity in implementing, but it has not an ability for considering the conjunction in substrates (Kolahchi *et al*. 2016). In order to improve the aforesaid weakness, a shear layer was attached over the spring series, known as Pasternak model. Application of Pasternak foundation on the post-buckling of FG porous nanobeam was analyzed by (Barati and Zenkour, 2017). The electro-mechanical vibration of FG plates with Pasternak foundation was investigated using four variable refined plate theory by Barati *et al*. (2017). Shafiei *et al*. (2016) and Rad and Shariyat (2015) showed that the trend of frequency for variation of porosity volume fraction is dependent on the values of power-law index value and foundation stiffness. Buckling, bending, and free vibration responses of FGM beams with porosities resting on an elastic foundation was examined by (Atmane *et al*. 2017). In that work, the authors presented closed form solutions utilizing Navier solution method. Recently, (Shahsavari *et al*. 2017a) developed even, uneven, log-uneven porosity distribution for quasi-3D vibration of FG plates rested on Winkler-Pasternak-Kerr elastic foundations using Galerkin method. From the above, it can be seen that there are many inconsistencies in porosity effect for different types of elastic foundation, especially at nanoscale. In this study, Kerr elastic foundation is considered herein for the sake of generalization.

In the current article, thermal buckling analysis of imperfect functionally graded nanobeam including porosities and piezoelectric layers when embedded in an elastic Kerr foundation is studied by using an analytic model based on the nonlocal elasticity theory (NET) and higher-order shear deformation beam theory. The NET is utilized to take the size-dependent effects and their equations are derived by using higher-order shear deformation beam theory. Material properties of FG nanobeams are supposed to be temperature-dependent and vary through the thickness direction and are determined through the modified power-law rule. Here the porosities with even type are considered. Applying Hamilton's principle, governing equations of higher-order FG nanobeam are obtained and solved by applying an analytical solution method. Uniform and nonlinear temperature distributions are also considered. Several numerical exercises indicate that various parameters such as nonlocal parameter, thickness ratio, type of temperature distribution, external electric voltage, porosity volume fraction, power-law index, and elastic Kerr foundation parameters have remarkable influence on the critical temperature of porous FG nanobeam.

2. Theory and formulation

In this study, we consider a smart porous functionally graded nanobeam, which is a nanosized sandwich beam with length L (in x-direction), width b (in y-direction) and thickness $h+2h_a$ (in z-direction), as shown in Fig. 1.

The core of the sandwich nanobeam is made of porous FG material with its properties varying smoothly across the thickness direction (the thickness is h), and is integrated with piezoelectric layers on its both sides (each piezoelectric layer has the thickness of h_a). The piezoelectric layers can be viewed as a piezoelectric sensor and a piezoelectric actuator, and the voltage V_a is applied to the piezoelectric actuator. Furthermore, the smart nanobeam is imbedded on an elastic medium, which is supposed to be modelled by using Kerr model (Kneifati 1985).

2.1 Numerical simulation procedure

By using the modified mixture rule, the effective material properties (P_f) of the evenly porous FGM core of the sandwich nanobeam can be expressed as (Wattanasakulpong and Ungbhakorn 2014)

$$P_f = P_u(V_u - \xi/2) + P_l(V_l - \xi/2) \tag{1}$$

where ξ is the volume fraction of even porosities. Notice that ξ is set to zero for a perfect FGM. Often the porosity is not even pattern, however, the rigorous requires a substantial work, which deserves further systematic investigations. P_u and P_l denote, respectively, the material properties of the top and bottom sides of the porous functionally graded core. V_u and V_l denote the volume fraction of top and bottom surfaces of the porous functionally graded core, respectively. In the case of a two-constituent and perfect FG material, we have

$$V_u + V_l = 1 \tag{2}$$

The effective material properties in the thickness are usually assumed to obey a power-law function (Dai *et al*. 2016, Li and Hu 2017a, b). Accordingly, the volume fraction of upper side (V_u) is defined as follows

$$V_u = \left(z/h + 0.5\right)^n \tag{3}$$

where the non-negative parameter n is called power-law exponent or the volume fraction index, and determines the material distribution across the thickness direction. According to Eqs. (1) and (2) and taking into the even

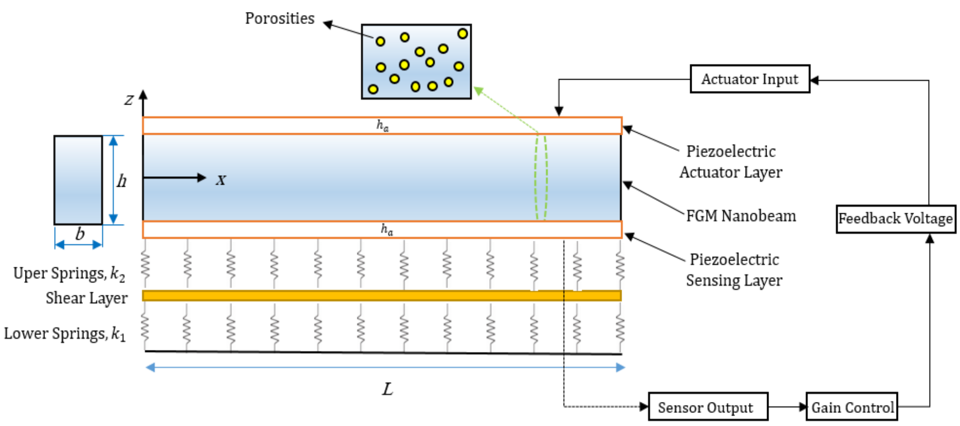

Fig. 1 Geometry of the FGM piezoelectric beam resting on elastic Kerr foundation

porosity effect account, the effective material properties of porous functionally graded core can be expressed as the following form

$$P(z)=(P_u-P_l)(z/h+0.5)^n+P_l-(P_u+P_l)(\xi/2) \quad (4)$$

In order to examine the behavior of the FGMs under high temperature more precisely, it is necessary to consider the temperature dependency on material properties. The temperature-dependent material properties of material phases can be written as (She *et al*. 2017a, Touloukian and Buyco 1970)

$$\mathrm{P}=\mathrm{P}_0(\mathrm{P}_{-1}\mathrm{T}^{-1}+\mathrm{P}_1\mathrm{T}+\mathrm{P}_2\mathrm{T}^2+\mathrm{P}_3\mathrm{T}^3+1) \quad (5)$$

where P_0, P_{-1}, P_1, P_2 and P_3 are the temperature-dependent coefficients. In this paper, the temperature-dependent coefficients are given in Table 1 for a two-constituent FGM made of Si_3N_4 and SUS304. Here the bottom and top surfaces of the porous functionally graded core are fully metal (SUS304) and fully ceramic (Si_3N_4), respectively. And we assume that the temperature varies through the thickness of nanobeam where $T(0.5h)=T_c$ and $T(-0.5h)=T_m$. As usual, we assume that all the material properties have the same form of function with respect to temperature T. It may be unreasonable and requires a substantial work, which deserves further systematic investigations.

2.2 Kinematic relations

Based on a Reddy's higher-order shear deformation theory (or second-order shear deformation theory), the displacement field at any point of the beam can be expreesed as (Khdeir and Reddy 1999)

$$u=u_0+z\phi_1+z^2\phi_2,\ w=w_0 \quad (6)$$

where u_0 and w_0 are the displacement components of the material point at the middle plane of the beam in the x-, and z-direction respectively; ϕ_1 and ϕ_2 are the rotation and variable of the higher-order terms, respectively. It has been reported by (Karami *et al*. 2018f) that the second-order shear deformation theory can be used to model nanoscale graphene and can reasonably interpret the dynamic behaviors of mounted graphene.

All displacement components (u_0, w_0, ϕ_1, ϕ_2) are dependent of x and time t. In addition, the nonzero strains of the higher-order shear deformation beam theory are expressed as

$$\begin{Bmatrix}\varepsilon_{xx}\\ \gamma_{xz}\end{Bmatrix}=\begin{Bmatrix}\varepsilon^0_{xx}\\ \gamma^0_{xz}\end{Bmatrix}+z\begin{Bmatrix}\varepsilon'_{xx}\\ \gamma'_{xz}\end{Bmatrix}+z^2\begin{Bmatrix}\varepsilon''_{xx}\\ \gamma''_{xz}\end{Bmatrix} \quad (7)$$

in which

$$\begin{Bmatrix}\varepsilon^0_{xx}\\ \gamma^0_{xz}\end{Bmatrix}=\begin{Bmatrix}\partial u_0/\partial x\\ \phi_1+\dfrac{\partial w_0}{\partial x}\end{Bmatrix},\begin{Bmatrix}\varepsilon'_{xx}\\ \gamma'_{xz}\end{Bmatrix}=\begin{Bmatrix}\dfrac{\partial\phi_1}{\partial x}\\ 2\phi_2\end{Bmatrix},\begin{Bmatrix}\varepsilon''_{xx}\\ \gamma''_{xz}\end{Bmatrix}=\begin{Bmatrix}\dfrac{\partial\phi_2}{\partial x}\\ 0\end{Bmatrix} \quad (8)$$

2.3 Constitutive equation based on nonlocal elasticity theory

The essence of the nonlocal elasticity theory is that, the stress field at a reference point x in an elastic continuum depends not only on strain at that point, but also on strains at all other points in the domain of interest (Lim *et al*. 2010, Pradhan and Murmu 2010, Wang and Duan 2008, Yang *et al*. 2010). Therefore, the nonlocal stress tensor σ_{ij} at the reference point x can be defined as follows (Lim *et al*. 2010, Pradhan and Murmu 2010, Wang and Duan 2008, Yang *et al*. 2010)

$$\tau_{ij}(x)=\int\alpha(|x'-x|,\tau)\sigma_{ij}(x')dV' \quad (9)$$

$$\sigma_{ij}(x)=C_{ijkl}(x)\varepsilon_{kl}(x) \quad (10)$$

here $\sigma_{ij}(x')$ is the classical (local) stress tensor at neighboring points x'. The scalar function α ($|x'-x|$, τ) is called the *nonlocal kernel function* which decays rapidly with the increase of the distance $|x'-x|$. $C_{ijkl}(x)$ is the fourth-order elasticity coefficient at the reference point x. And τ is defined by $\tau=e_0a/l$ where the term (e_0a) is the nonlocal parameter. The difference between the classical and nonlocal elasticity theories lies in the presence of small scale parameter e_0a in the nonlocal theory (Lim *et al*. 2010, Pradhan and Kumar 2011, Pradhan and Murmu 2010, Wang and Duan 2008, Yang *et al*. 2010). Notice that the internal characteristic length a is often determined based on lattice parameter, granular size, bond length, and so on, and e_0 is a material constant which is often determined from

Table 1 Temperature-dependent coefficients for stainless steel and silicon nitride

Properties	Material	P_0	P_{-1}	P_1	P_2	P_3
κ (W/mK)	Stainless Steel	15.379	0	-1.264×10^{-3}	2.092×10^{-6}	-7.223×10^{-10}
	Silicon Nitride	13.723	0	-1.032×10^{-3}	5.466×10^{-6}	-7.876×10^{-11}
α (/K)	Stainless Steel	12.330×10^{-6}	0	8.086×10^{-4}	0	0
	Silicon Nitride	5.8723×10^{-6}	0	9.095×10^{-4}	0	0
v	Stainless Steel	0.3262	0	-2.002×10^{-4}	3.797×10^{-7}	0
	Silicon Nitride	0.2400	0	0	0	0
E (Pa)	Stainless Steel	201.04×10^9	0	3.079×10^{-4}	-6.534×10^{-7}	0
	Silicon Nitride	348.43×10^9	0	-3.070×10^{-4}	2.160×10^{-7}	-8.946×10^{-11}

experimental data or atomic lattice dynamics (Zhu and Li 2017a, b). The external characteristic length l is often determined based on crack length, wavelength and so on.

It is often quite difficult to analyze the governing equations based on the integral nonlocal constitutive equation. Hence, for unbounded domain problems, the strain-driven nonlocal integral model (Eq. (9)) equipped with Helmholtz averaging kernel can be equivalently transformed as a nonlocal differential model as follow (Eringen 1983)

$$(1-\mu^2\nabla^2)\sigma_{ij} = C_{ijkl}\varepsilon_{kl} \tag{11}$$

in which $\mu = (e_0a)^2$, and ∇^2 is the Laplacian operator in Cartesian coordinate. As shown by Eringen in his original paper (Eringen 1983), the nonlocal model (11) is so-called Eringen Nonlocal Differential Model (ENDM). The ENDM can be easily applied and consequently has been extensively used in nanotechnology (Arash and Wang 2012, Li and Hu 2017b, Peddieson *et al*. 2003, Wang and Wang 2007). Nevertheless, when considering boundary condition problems, the nonlocal integral and differential models (Eqs. (9) and (11)) are not usually equivalent to each other since constitutive boundary conditions on the stress naturally appear in dealing with bounded domains (Barretta *et al*. 2018a, b, Romano and Barretta 2017, Romano *et al*. 2017a, b). The ENDM can be viewed as a phenomenological model or a stress gradient model, which has been proved to show good agreement with molecular dynamic results (Hu *et al*. 2008, Murmu and Adhikari 2012, Wang and Hu 2008).

To capture small-scale effects, the nonlocal differential constitutive equation is used herein. Therefore, the size-dependent constitutive equation of the smart porous FG nanobeam incorporating the thermal and piezoelectric effects can be expressed as (Mirzavand and Eslami 2011, Nami *et al*. 2015)

$$\begin{aligned}&\begin{Bmatrix}\sigma_{xx}\\ \tau_{xz}\end{Bmatrix}-\mu\nabla^2\begin{Bmatrix}\sigma_{xx}\\ \tau_{xz}\end{Bmatrix}=\begin{bmatrix}C_{11} & 0\\ 0 & C_{55}\end{bmatrix}\left(\begin{Bmatrix}\varepsilon_{xx}\\ \gamma_{xz}\end{Bmatrix}-\begin{Bmatrix}\alpha\\ 0\end{Bmatrix}\theta\right)\\ &-\begin{bmatrix}0 & e_{31}\\ e_{15} & 0\end{bmatrix}\begin{Bmatrix}E_x\\ E_z\end{Bmatrix}\end{aligned} \tag{12}$$

where θ is the temperature difference. And C_{ij} is the elastic stiffness of the FGM core of the smart sandwich beam and can be given by

$$C_{11} = \frac{E(z)}{1-\upsilon^2}, C_{55} = \frac{E(z)}{2(1+\upsilon)} \tag{13}$$

The piezoelectric stress constants e_{31}, e_{15} can be expressed in terms of the dielectric constants (or piezoelectric strain constants) d_{31}, d_{15} and the elastic constants $C_{ij}^{(a)}$ of the piezoelectric actuator layers as (Mirzavand and Eslami 2011)

$$e_{31} = d_{31}C_{11}^a, e_{15} = d_{15}C_{55}^a \tag{14}$$

The longitudinal component of electric field E_x is negligible, and the transverse component of electric field E_z is dominant in the beam-type piezoelectric material. Thus, we can assume that

$$E_z = V_a/h_a, E_x = 0 \tag{15}$$

here V_a and h_a are the electric voltage applied to the piezoelectric actuator in the thickness direction and the thickness of the piezoelectric actuator, respectively.

2.4 Governing equations

Using Hamilton's praincipile, the equation of motion will be drived by

$$\int_0^t \delta(U+V-K)dt = 0 \tag{16}$$

Here U is strain energy, V is work done by external forces and K is kinetic energy. The virtual variation of strain energy can be written as

$$\delta U = \int_v \sigma_{ij}\delta\varepsilon_{ij}dV = \int_v \left[\sigma_{xx}\delta\varepsilon_{xx} + \tau_{xz}\delta\gamma_{xz}\right]dV \tag{17}$$

Substituting Eqs. (11) and (12) into Eq. (17) yields

$$\begin{aligned}\delta U = \int_0^L \Bigg[& N_x\frac{\partial\delta u}{\partial x} + M_x\frac{\partial\delta\phi_1}{\partial x} + L\frac{\partial\delta\phi_2}{\partial x}\\ & -Q_{xz}\left(\phi_1 + \frac{\partial w}{\partial x}\right) - 2R_{xz}(\phi_2)\Bigg]dx\end{aligned} \tag{18}$$

in which the stress resultants are defined as

$$\begin{aligned}&\begin{Bmatrix}\{N\}\\ \{M\}\\ \{L\}\end{Bmatrix}=\begin{bmatrix}[A] & [B] & [C]\\ [B] & [C] & [D]\\ [C] & [D] & [E]\end{bmatrix}\begin{Bmatrix}\{\varepsilon_{xx}^0\}\\ \{\varepsilon'_{xx}\}\\ \{\varepsilon''_{xx}\}\end{Bmatrix}\\ &\begin{Bmatrix}\{Q\}\\ \{R\}\end{Bmatrix}=\begin{bmatrix}[A] & [B]\\ [B] & [C]\end{bmatrix}\begin{Bmatrix}\{\gamma_{xz}^0\}\\ \{\gamma'_{xz}\}\end{Bmatrix}\end{aligned} \tag{19}$$

where

$$(A_{ij}, B_{ij}, C_{ij}, D_{ij}, E_{ij}) = \int_{-h/2}^{h/2} \sigma_{ij}(1, z, z^2, z^3, z^4)dz \tag{20}$$

The first variation of work done by applied forces can be written in the form

$$\delta V = \int_0^L \left[N_{xx}^0\left(\frac{\partial w}{\partial x}\frac{\partial\delta w}{\partial x}\right) + q_{\mathrm{Kerr}}\delta w\right]dx \tag{21}$$

here N_{xx}^0 is the axial compressing force. The distributed reaction q_{Kerr} of the Kerr medium can be expressed as (Kneifati 1985)

$$q_{\mathrm{Kerr}} - \left(\frac{k^s}{k_1+k_2}\right)\nabla^2 q_{\mathrm{Kerr}} = \left(\frac{k_1k_2}{k_1+k_2}\right)w - \left(\frac{k^sk_2}{k_1+k_2}\right)\nabla^2 w \tag{22}$$

The Kerr foundation model consists of a shear layer (with stiffness k^s) attached to two independent upper and lower elastic layers (modeled by distributed springs) with stiffness of k_2 and k_1, respectively.

The variation of kinetic energy is represented by

$$\delta K = \int_\Omega \int_{-\frac{h}{2}}^{\frac{h}{2}} \rho(z,t)(\frac{\partial u}{\partial t}\frac{\delta\partial u}{\partial t} + \frac{\partial w}{\partial t}\frac{\delta\partial w}{\partial t})dzd\Omega$$

$$= \int_0^L (I_0(\frac{\partial u_0}{\partial t}\frac{\delta\partial u_0}{\partial t} + \frac{\partial w_0}{\partial t}\frac{\delta\partial w_0}{\partial t}) + I_1(\frac{\partial u_0}{\partial t}\frac{\delta\partial \phi_1}{\partial t} + \frac{\partial \phi_1}{\partial t}\frac{\delta\partial u_0}{\partial t}) \quad (23)$$

$$+I_2(\frac{\partial u_0}{\partial t}\frac{\delta\partial \phi_2}{\partial t} + \frac{\partial \phi_1}{\partial t}\frac{\delta\partial \phi_1}{\partial t} + \frac{\partial \phi_2}{\partial t}\frac{\delta\partial u_0}{\partial t})$$

$$+I_3(\frac{\partial \phi_1}{\partial t}\frac{\delta\partial \phi_2}{\partial t} + \frac{\partial \phi_2}{\partial t}\frac{\delta\partial \phi_1}{\partial t}) + I_4(\frac{\partial \phi_2}{\partial t}\frac{\delta\partial \phi_2}{\partial t})dx$$

where

$$(I_0, I_1, I_2, I_3, I_4) = \int_{-h/2}^{h/2} (1, z, z^2, z^3, z^4)\rho(z)dz \quad (24)$$

The governing equations are obtained by inserting Eqs. (18)-(23) in Eq. (16) when the coefficients of δu, δw, $\delta\phi_1$ and $\delta\phi_2$ are equal to zero.

$$\frac{\partial N_{xx}}{\partial x} = I_0\frac{\partial^2 u}{\partial t^2} + I_1\frac{\partial^2 \phi_1}{\partial t^2} + I_2\frac{\partial^2 \phi_2}{\partial t^2} \quad (25)$$

$$\frac{\partial Q_{xz}}{\partial x} + N_{xx}^0\frac{\partial^2 w}{\partial x^2} - \frac{k_1 k_2}{k_1+k_2}w + \frac{k^s k_2}{k_1+k_2}\frac{\partial^2 w}{\partial x^2} = I_0\frac{\partial^2 w}{\partial t^2} \quad (26)$$

$$\frac{\partial M_{xx}}{\partial x} - Q_{xz} = I_1\frac{\partial^2 u}{\partial t^2} + I_2\frac{\partial^2 \phi_1}{\partial t^2} + I_3\frac{\partial^2 \phi_2}{\partial t^2} \quad (27)$$

$$\frac{\partial L_{xx}}{\partial x} - 2R_{xz} = I_2\frac{\partial^2 u}{\partial t^2} + I_3\frac{\partial^2 \phi_1}{\partial t^2} + I_4\frac{\partial^2 \phi_2}{\partial t^2} \quad (28)$$

According to the size-dependent constitutive equation of the smart porous FG nanobeam incorporating the thermal and piezoelectric effects, the stress resultants can be expressed as

$$N_{xx} - \mu\nabla^2(N_{xx}) = A_{11}\frac{\partial u_0}{\partial x} + B_{11}\frac{\partial \phi_1}{\partial x} + D_{11}\frac{\partial \phi_2}{\partial x} - G_{11} - J_1 \quad (29)$$

$$M_{xx} - \mu\nabla^2(M_{xx}) = B_{11}\frac{\partial u_0}{\partial x} + D_{11}\frac{\partial \phi_1}{\partial x} + E_{11}\frac{\partial \phi_2}{\partial x} - H_{11} - J_2 \quad (30)$$

$$L_{xx} - \mu\nabla^2(L_{xx}) = D_{11}\frac{\partial u_0}{\partial x} + E_{11}\frac{\partial \phi_1}{\partial x} + F_{11}\frac{\partial \phi_2}{\partial x} - Y_{11} - J_3 \quad (31)$$

$$\phi_{xz} - \mu\nabla^2(Q_{xz}) = A_{55}(\phi_1 + \partial w_0/\partial x) + B_{55}(2\phi_2) \quad (32)$$

$$R_{xz} - \mu\nabla^2(R_{xz}) = B_{55}(\phi_1 + \partial w_0/\partial x) + D_{55}(2\phi_2) \quad (33)$$

where

$$G_{ij} = \int_{-h/2-h_a}^{h/2+h_a} (C_{ij}\alpha\theta)dz,\ H_{ij} = \int_{-\frac{h}{2}-h_a}^{\frac{h}{2}+h_a} (C_{ij}\alpha\theta)zdz, \quad (34)$$

$$Y_{ij} = \int_{-h/2-h_a}^{h/2+h_a} (C_{ij}\alpha\theta)z^2dz, (J_1, J_2, J_3) = \int_{-h/2-h_a}^{h/2+h_a} e_{31}E_z(1, z, z^2) \quad (34)$$

Substituting Eqs (29)-(33) and Eqs. (34) into Hamilton's prainciple (16), the governing equations including the effects of thermal environment and piezoelectric layers can be obtained as

$$A_{11}\frac{\partial^2 u_0}{\partial x^2} + B_{11}\frac{\partial^2 \phi_1}{\partial x^2} + D_{11}\frac{\partial^2 \phi_2}{\partial x^2} - \frac{\partial}{\partial x}G_{11} - \frac{\partial J_1}{\partial x} = (1-\mu\nabla^2)(I_0\frac{\partial^2 u}{\partial t^2} + I_1\frac{\partial^2 \phi_1}{\partial t^2} + I_2\frac{\partial^2 \phi_2}{\partial t^2}) \quad (35)$$

$$A_{55}\left(\frac{\partial \phi_1}{\partial x} + \frac{\partial^2 w_0}{\partial x^2}\right) + 2B_{55}\frac{\partial \phi_2}{\partial x} + (1-\mu\nabla^2)(N_{xx}^0\frac{\partial^2 w_0}{\partial x^2} - \frac{k_1k_2}{k_1+k_2}w_0 + \frac{k_2k^s}{k_1+k_2}\frac{\partial^2 w_0}{\partial x^2}) = (1-\mu\nabla^2)I_0\frac{\partial^2 w}{\partial t^2} \quad (36)$$

$$B_{11}\frac{\partial^2 u_0}{\partial x^2} + D_{11}\frac{\partial^2 \phi_1}{\partial x^2} + E_{11}\frac{\partial^2 \phi_2}{\partial x^2} - \frac{\partial}{\partial x}H_{11} - \frac{\partial J_2}{\partial x} = (1-\mu\nabla^2)(I_1\frac{\partial^2 u}{\partial t^2} + I_2\frac{\partial^2 \phi_1}{\partial t^2} + I_3\frac{\partial^2 \phi_2}{\partial t^2}) \quad (37)$$

$$D_{11}\frac{\partial^2 u_0}{\partial x^2} + E_{11}\frac{\partial^2 \phi_1}{\partial x^2} + F_{11}\frac{\partial^2 \phi_2}{\partial x^2} - \frac{\partial}{\partial x}Y_{11} - \frac{\partial J_3}{\partial x} - 2B_{55}\left(\phi_1 + \frac{\partial w_0}{\partial x}\right) - 4D_{55}\phi_2 = (1-\mu\nabla^2)(I_2\frac{\partial^2 u}{\partial t^2} + I_3\frac{\partial^2 \phi_1}{\partial t^2} + I_4\frac{\partial^2 \phi_2}{\partial t^2}) \quad (38)$$

3. Solution procedures

In this section, an analytical approach will be used to solve the nonlocal governing equations of functionally graded nanobeam with simply-supported boundary edge. To satisfy this boundary condition, the following Navier-series are intended for displacement variables

$$u = \sum_{m=1}^{\infty} U_m \cos\alpha x e^{i\omega t} \quad (39)$$

$$w = \sum_{m=1}^{\infty} W_m \sin\alpha x e^{i\omega t} \quad (40)$$

$$\phi_1 = \sum_{m=1}^{\infty} \Phi_{1m} \cos\alpha x e^{i\omega t} \quad (41)$$

$$\phi_2 = \sum_{m=1}^{\infty} \Phi_{2m} \cos\alpha x e^{i\omega t} \quad (42)$$

where m denotes the number of half waves in x- direction; $\alpha = \frac{m\pi}{L}$; (U_m, W_m, Φ_{1m}, Φ_{2m}) denote constant coefficients that depend on m. Substituting Eqs. (39)-(42) into the equations of motion (Eqs. (35)-(38)), respectively, leads to Eqs. (43)-(46)

$$\begin{aligned}&(-A_{11}(\frac{m\pi}{L})^2+I_0(1+\mu(\frac{m\pi}{L})^2)\omega_n^2)U_m\\&+(-B_{11}(\frac{m\pi}{L})^2+I_1(1+\mu(\frac{m\pi}{L})^2)\omega_n^2)\Phi_{1m}\\&+(-D_{11}(\frac{m\pi}{L})^2+I_2(1+\mu(\frac{m\pi}{L})^2)\omega_n^2)\Phi_{2m}\\&-G_{11}\frac{m\pi}{L}-J_1\frac{m\pi}{L}=0\end{aligned} \tag{43}$$

$$\begin{aligned}&(-A_{55}\frac{m\pi}{L})\Phi_{1m}+(-A_{55}(\frac{m\pi}{L})^2\\&+I_0(1+\mu(\frac{m\pi}{L})^2)\omega_n^2)-N_{xx}^0(\frac{m\pi}{L})^2(1+\mu(\frac{m\pi}{L})^2)\\&+(-\frac{k_1k_2}{k_1+k_2}-\frac{k_2k^s}{k_1+k_2}(\frac{m\pi}{L})^2)(1+\mu(\frac{m\pi}{L})^2))W_m\\&+(-2B_{55}\frac{m\pi}{L})\Phi_{2m}=0\end{aligned} \tag{44}$$

$$\begin{aligned}&(-B_{11}(\frac{m\pi}{L})^2+I_1(1+\mu(\frac{m\pi}{L})^2)\omega_n^2))U_m\\&+(-D_{11}(\frac{m\pi}{L})^2+I_2(1+\mu(\frac{m\pi}{L})^2)\omega_n^2))\Phi_{1m}\\&+(-E_{11}(\frac{m\pi}{L})^2+I_3(1+\mu(\frac{m\pi}{L})^2)\omega_n^2))\Phi_{2m}\\&-H_{11}\frac{m\pi}{L}-J_2\frac{m\pi}{L}=0\end{aligned} \tag{45}$$

$$\begin{aligned}&(-D_{11}(\frac{m\pi}{L})^2+I_2(1+\mu(\frac{m\pi}{L})^2)\omega_n^2))U_m\\&+(-E_{11}(\frac{m\pi}{L})^2-2B_{55}+I_3(1+\mu(\frac{m\pi}{L})^2)\omega_n^2))\Phi_{1m}\\&+(-2B_{55}\frac{m\pi}{L})W_m+(-F_{11}(\frac{m\pi}{L})^2-4D_{55}\\&+I_4(1+\mu(\frac{m\pi}{L})^2)\omega_n^2))\Phi_{2m}-Y_{11}\frac{m\pi}{L}-J_3\frac{m\pi}{L}=0\end{aligned} \tag{46}$$

By setting the determinant of the coefficient matrix of the above equations, the analytical solutions can be obtained from the following equations

$$\left\{([\mathrm{K}]+\Delta T\,[\mathrm{K_T}])\right\}-\omega^2[\mathrm{M}]\begin{Bmatrix}U_m\\ \Phi_{1m}\\ \Phi_{2m}\\ W_m\end{Bmatrix}=0 \tag{47}$$

in which $[K]$ and $[K_T]$ respectively, denote stiffness matrix and the coefficient matrix of temperature change, and $[M]$ denotes the mass matrix. By setting this polynomial to zero, we can find natural frequencies ω_n and critical buckling temperature ΔT_{cr}.

The aim of the presented paper is to investigate the two types of temperature distributions across thickness (namely uniform and nonlinear temperature distributions). It is important to know, for the uniform temperature case, the assumed structure will be exposed to a constant; but for the nonlinear case, the temperature will change across the thickness direction of the structure. For the nonlinear temperature rise, the equation referred to the heat transfer may be described as follow (Mirzavand and Eslami 2011)

$$\frac{d}{dz}\left[\kappa(z)\frac{dT}{dz}\right]=0 \quad \text{at} \quad x=0,L \tag{48}$$

4. Numerical results and discussions

In this section, the effect of two type of temperature change namely uniform and nonlinear, material composition, porosities, nonlocality effect, voltage, elastic Kerr foundation and thickness on the thermal buckling response of porous functionally graded (FG) nanobeam will be figured out. The beam geometry has the following dimensions: L (length) = 10 nm, b (width) = 1 nm and h (thickness) is variable. In addition, the following non-dimensional parameters are used to describe the numerical results in graphical and tabular forms are defined as

$$\tilde{\omega}=\omega L^2\sqrt{\rho_c A/E_c I},\ \Delta T_{cr}=1000\alpha_c\Delta \mathrm{T}$$

$$\mathrm{K}_1=\frac{k_1L^4}{D_{11}}\mathrm{K}_2=\frac{k_2L^4}{D_{11}},\mathrm{K}^s=\frac{k^sL^2}{D_{11}},D_{11}=\frac{E_ch^3}{12(1-\nu_c{}^2)}$$

4.1 Validation

Consider a functionally graded beam with fully simply supported boundary conditions subjected to nonlocality effect. In Table 2 results are shown for different power-law indices n. The present results are compared with finite element method on the basis of Euler-Bernoulli beam theory and analytical method on the basis of Reddy's shear deformation beam theory. In this case, it can be observed

Table 2 Comparison of the nondimensional fundamental frequency $\tilde{\omega}$ for a S-S FG nanobeam with various gradient indexes when L = 10 nm, h = 0.5 nm

	n = 0		n = 0.2		n = 0.5		n = 1		n = 5	
μ (nm^2)	(Eltaher Emam *et al.* 2012)	Present	(Eltaher Emam *et al.* 2012)	Present	(Eltaher Emam *et al.* 2012)	Present	(Eltaher Emam *et al.* 2012)	Present	(Eltaher Emam *et al.* 2012)	Present
0	9.8797	10.1291	8.7200	8.8546	7.8061	7.7818	7.0904	7.0179	6.0025	6.0018
1	9.4238	9.6634	8.3175	8.4475	7.4458	7.4241	6.7631	6.6953	5.7256	5.7259
2	9.0257	9.2566	7.9661	8.0919	7.1312	7.1115	6.4774	6.4134	5.4837	5.4848
3	8.6741	8.8972	7.6557	7.7777	6.8533	6.8354	6.2251	6.1644	5.2702	5.2718
4	8.3607	8.5766	7.3791	7.4975	6.6057	6.5891	6.0001	5.9423	5.0797	5.0819
5	8.0789	8.2884	7.1303	7.2455	6.3830	6.3677	5.7979	5.7426	4.9086	4.9111

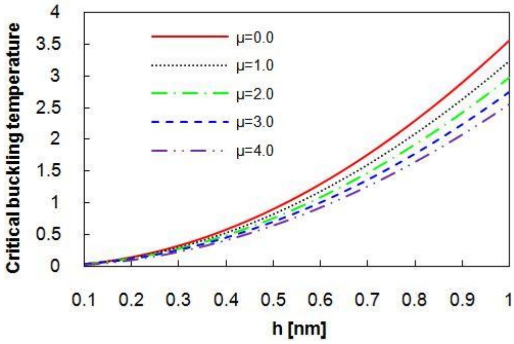

(a) Uniform

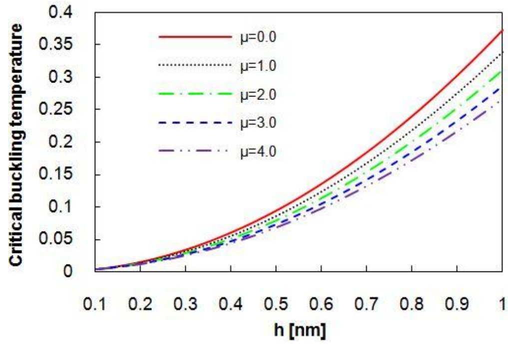

(b) Nonlinear

Fig. 2 Thermal buckling relation between critical temperature and thickness of imperfect FG nanobeam for different temperature distributions (L = 10 mm, n = 1, ξ = 0.2)

from Table 2 that the present results are in good agreement with available literature.

4.2 Role of nonlocal parameter on thermal buckling response

Thermal buckling response of simply supported porous FG nanobeam with respect to beam thickness for different values of nonlocal parameters under different temperature distributions namely uniform and nonlinear are depicted in Fig. 2. Given this figure, it is easily understood for an S-S porous FG nanobeam that, an increase in beam thickness parameter gives rise to an increase in the critical temperature (ΔT_{cr}). Also, it is observed that the with increases nonlocal parameter the results will decrease. In additions, it was concluded that the nonlocality effect is more efficient in thick and moderately thick FG beams in comparison with the thin ones.

4.3 Role of porosities on thermal buckling response

Thermal buckling responses of S-S FG nanobeam for different porosity coefficients and beam thickness under uniform and nonlinear temperature distributions are illustrated in Figs. 3 and 4, respectively at μ = 1.0 nm^2. It can be observed from these figures that with an increase of the porosity coefficient, critical temperature decreases. It is seen from Figs. 3 and 4 that the beam thickness shows an

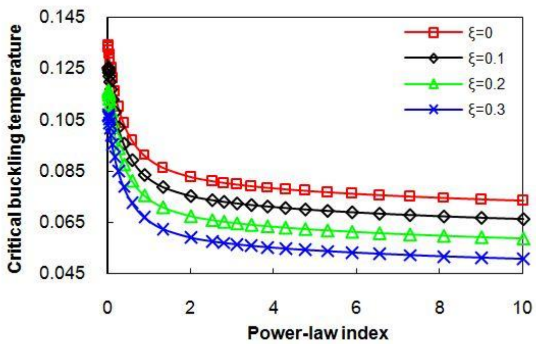

(a) h = 0.15 nm

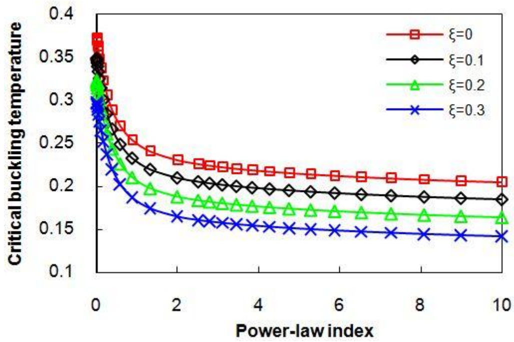

(b) h = 0.25 nm

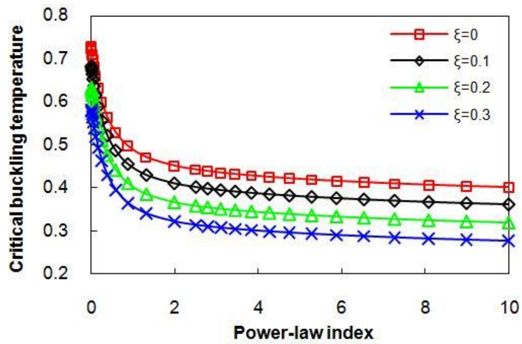

(c) h = 0.35 nm

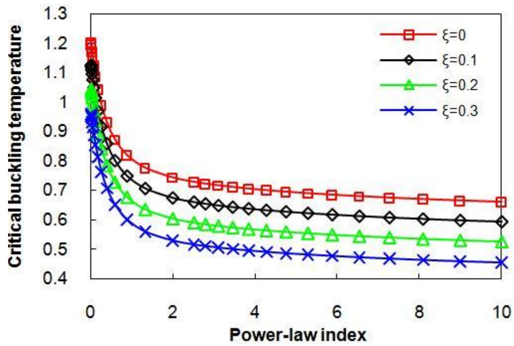

(d) h = 0.45 nm

Fig. 3 The variation of the critical temperature of FG nanobeam with material compositions and even porosity pattern for different beam thickness (uniform temperature distribution)

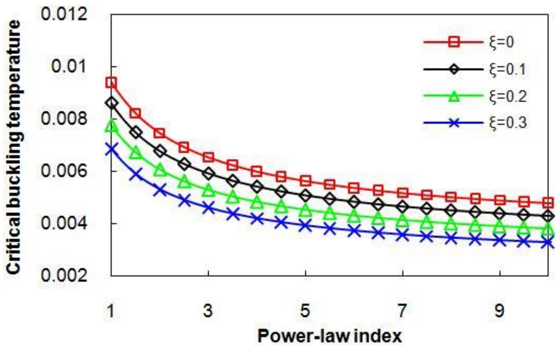

(a) h = 0.15 nm

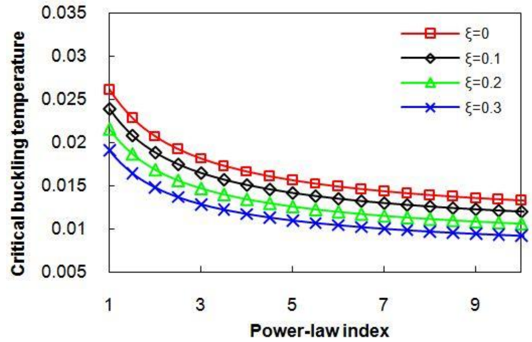

(b) h = 0.25 nm

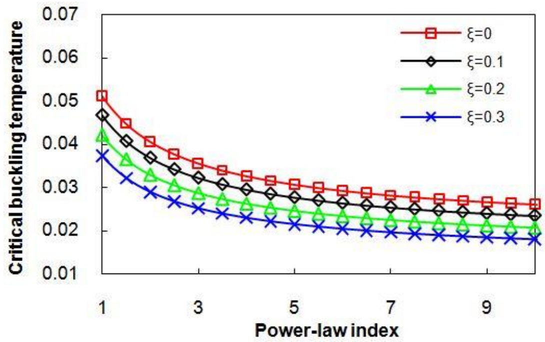

(c) h = 0.35 nm

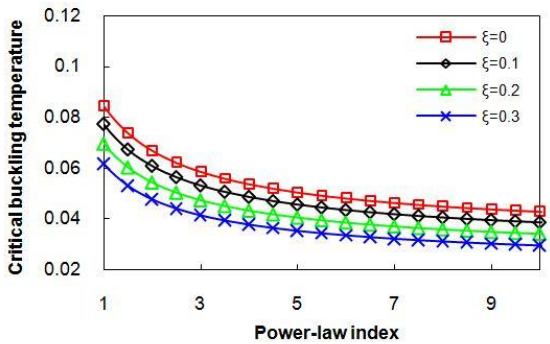

(d) h = 0.45 nm

Fig. 4 The variation of the critical temperature of FG nanobeam with material compositions and even porosity pattern for different beam thickness (nonlinear temperature distribution)

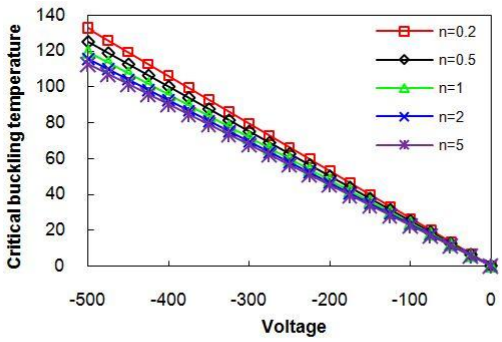

(a) h = 0.15 nm

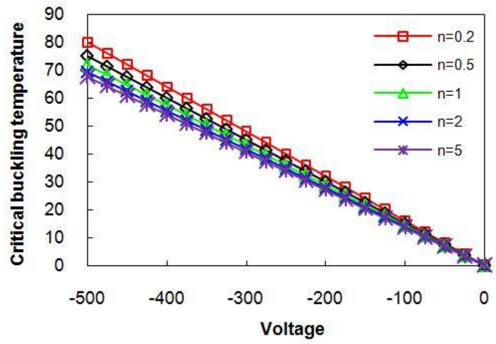

(b) h = 0.25 nm

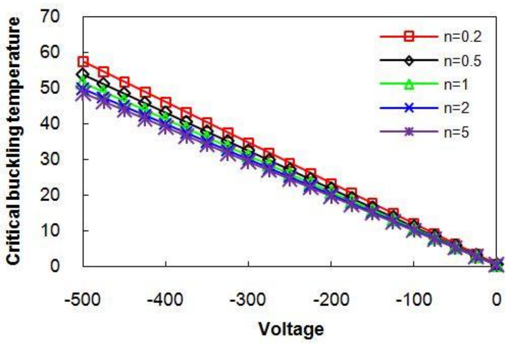

(c) h = 0.35 nm

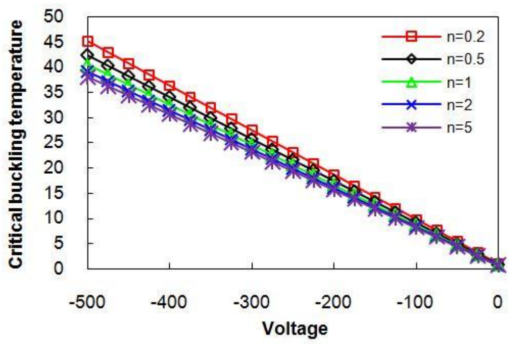

(d) h = 0.45 nm

Fig. 5 The effects of voltage and material compositions on the critical temperature for different thickness values (uniform temperature distribution) increasing effect on critical temperature for all values of power-law indexes. Also in Figs. 3 and 4 it is observed that porosity distribution decreases the critical temperature of imperfect FG nanobeam. Although, the influence of porosity on the results will be increased with increasing the power-law index.

4.4 Role of piezoelectric layers on thermal buckling

As another example to applying the external voltage effect on critical temperature of porous FG nanobeams under uniform and nonlinear temperature distribution, Figs. 5 and 6 are plotted for various values of beam thickness in versus power-law index at μ = 1.0 nm^2. To consideration the voltage effect it is assumed that functionally graded beam integrated with piezoelectric layers in both sides. So, for piezoelectric layers, G-1195N are considered which thickness of actuator layer is $h_a = 2\times10^{-12}$ m and G-1195N properties are $E_{11} = 63\times10^9$ Pa, $\upsilon_{12} = \upsilon_{21} = 0.3$ and $d_{31} = d_{32} = 1\times10^{-13}$ m/V. It is shown that critical temperature reduces with increase of voltage and power-law indices in all values of beam thicknesses. One can also understand that the results are varied linearly with respect to voltage. In addition, with respect to material compositions, the effect of power-law index to decrease results in lower value of voltage is more. By comparing these figures, it is observed that critical temperature for nonlinear temperature distribution are lower than those for uniform temperature

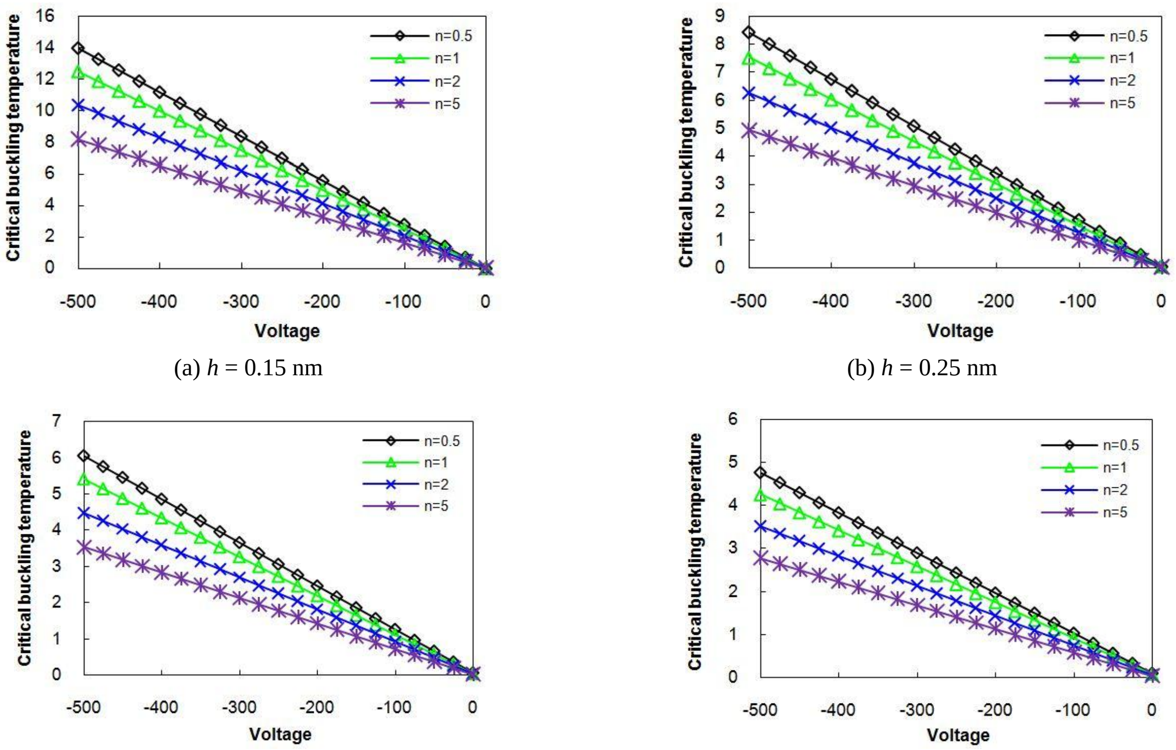

(a) h = 0.15 nm (b) h = 0.25 nm

(c) h = 0.35 nm (d) h = 0.45 nm

Fig. 6 The effects of voltage and material compositions on the critical temperature for different thickness values (nonlinear temperature distribution)

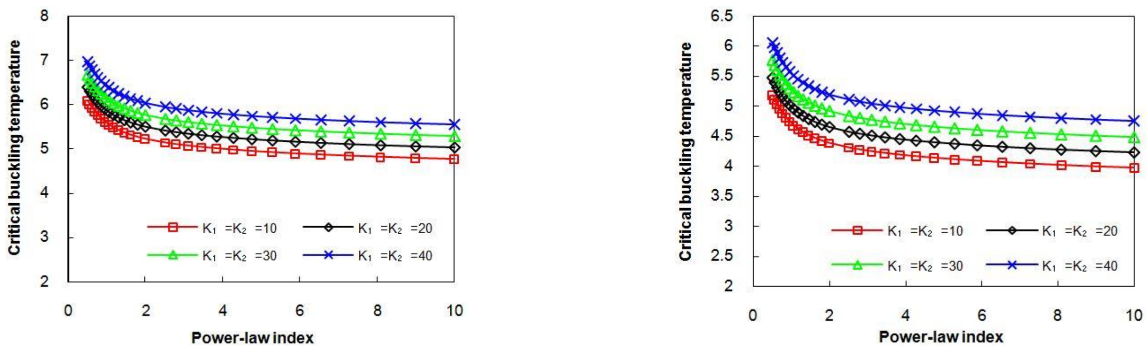

(a) $\xi = 0$ (b) $\xi = 0.2$

Fig. 7 Variation of critical temperature under uniform temperature distribution of mounted FG core versus material compositions for different values of linear layer of Kerr foundation (L / h = 10 mm, μ = 1.0, K^s = 5)

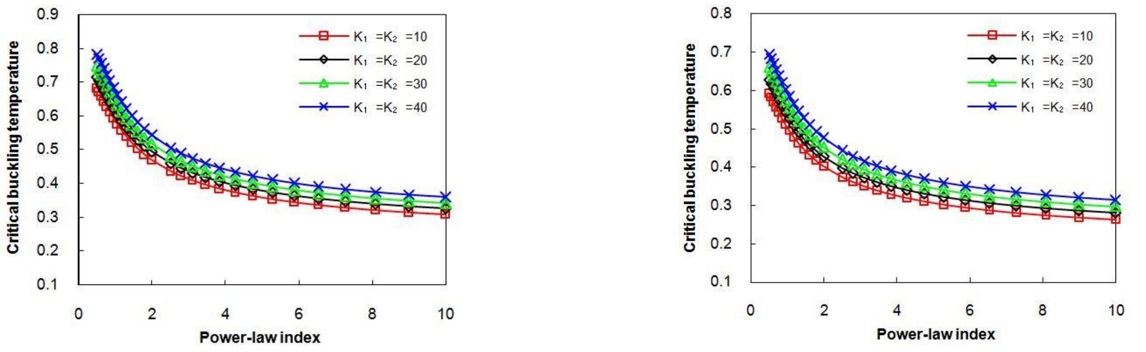

(a) $\xi = 0$ (b) $\xi = 0.2$

Fig. 8 Variation of critical temperature under nonlinear temperature distribution of mounted FG core versus material compositions for different values of linear layer of Kerr foundation (L / h = 10 mm, μ = 1.0, K^s = 5)

distribution.

4.5 Role of elastic Kerr foundation on thermal buckling response

Variation of critical temperature of mounted FG nanobeams versus power-law index under uniform temperature distribution for different values of linear layer of Kerr foundation illustrated in Fig. 7 at L/h = 10, K_s = 5 and μ = 1.0 nm^2. Also, Figs. 7(a) and (b) shows the behavior of perfect and imperfect FG nanobeams respectively. Simplicity assumption is based on that stiffness of upper and lower springs of Kerr foundation are identical. It was shown that the results increased by increasing the stiffness of springs. In fact, the nanobeam becomes more rigid by increasing the stiffness of springs loading. Also, it is concluded that the linear layer of foundation performs increasing effect on the results for imperfect FG nanobeam.

As another example, to study the effect of the linear layer of Kerr foundation on the thermal buckling response of FG nanobeams under nonlinear temperature distribution with and without porosities, the Fig. 8 is drawn. It is concluded that in perfect and imperfect FG nanobeams by increasing stiffness of springs, critical temperature will increase.

In order to consider the effect of shear layer of foundation Figs. 9 and 10 are drawn. It is obvious that with increasing shear layer of foundation, results for perfect and imperfect FG nanobeams under uniform and nonlinear temperature distribution will increase. Also, it is found that in the presence of elastic Kerr foundation, critical temperature reduces with the increase of porosity coefficients.

From Figs. 7-10, it can be observed that, for thermal buckling response of perfect and imperfect FG nanobeams under uniform and nonlinear temperature distribution for all values of elastic Kerr foundation the critical temperature reduces with the increase of gradient index, where this reduction is more sensible according to the lower values of gradient index. Also, it is concluded that the shear layer of the elastic Kerr foundation has a more remarkable effect on the critical temperature than linear layer parameters. In fact, with the increase of shear layer, the critical temperature increases significantly.

5. Conclusions

By considering nonlocal effects, the thermal buckling response of porous functionally graded core integrated with piezoelectric layers is studied for the first time based on a higher-order shear deformation beam model. Nanobeam is assumed to be rested on elastic Kerr foundation incorporating three coefficients. And a modified power-law

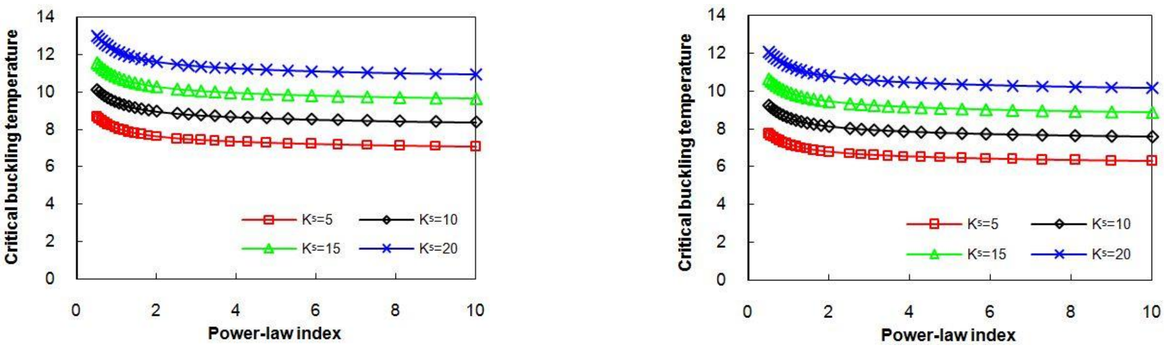

(a) $\xi = 0$ (b) $\xi = 0.2$

Fig. 9 Variation of critical temperature under uniform temperature distribution of mounted FG core versus material compositions for different values of shear layer of Kerr foundation (L / h = 10 mm, μ = 1.0, K^s = 5)

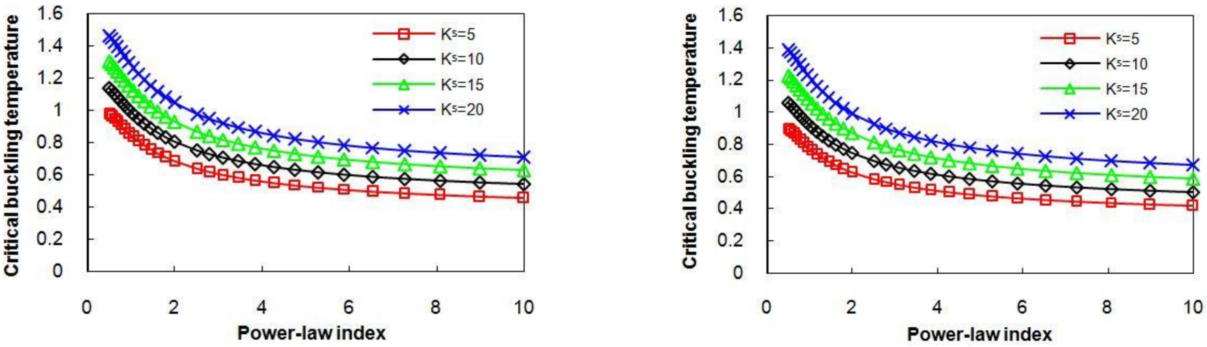

(a) $\xi = 0$ (b) $\xi = 0.2$

Fig. 10 Variation of critical temperature under nonlinear temperature distribution of mounted FG core versus material compositions for different values of shear layer of Kerr foundation (L / h = 10 mm, μ = 1.0, K^s = 5)

role is used to describe the material properties of the beam. Nonlocal elasticity theories together with Hamilton's principle are applied for obtaining the governing equations to analyze buckling behavior. Outlined discussions are given to show how to change the critical buckling temperatures by varying the thickness of beam, linear and shear stiffness coefficients of elastic Kerr foundation, porosity, power law index, temperature distribution, electric voltage and nonlocal parameter. The outcomes are presented for simply-supported sandwich beams. With relying on the results of the present investigation, the following considerations are valuable:

- The critical temperature decreases as nonlocal parameter increases.
- With the growth of beam thickness, the critical temperature increases.
- The critical temperature may decrease with respect to the increment of the power-law indices and porosity coefficients.
- The piezoelectric layer can reduce the critical buckling temperature.
- With the increment in the stiffness of linear and shear layers of elastic Kerr foundation, the functionally graded nanobeam will be more rigid and hence its critical temperature increases.

References

Ansari, R., Pourashraf, T., Gholami, R. and Shahabodini, A. (2016), "Analytical solution for nonlinear postbuckling of functionally graded carbon nanotube-reinforced composite shells with piezoelectric layers", *Compos. Part B: Eng.*, **90**, 267-277.

Arash, B. and Wang, Q. (2012), "A review on the application of nonlocal elastic models in modeling of carbon nanotubes and graphenes", *Computat. Mater. Sci.*, **51**(1), 303-313.

Atmane, H.A., Tounsi, A. and Bernard, F. (2017), "Effect of thickness stretching and porosity on mechanical response of a functionally graded beams resting on elastic foundations", *Int. J. Mech. Mater. Des.*, **13**(1), 71-84.

Barati, M.R. and Zenkour, A.M. (2017), "Investigating post-buckling of geometrically imperfect metal foam nanobeams with symmetric and asymmetric porosity distributions", *Compos. Struct.*, **182**, 91-98.

Barati, M.R., Shahverdi, H. and Zenkour, A.M. (2017), "Electro-mechanical vibration of smart piezoelectric FG plates with porosities according to a refined four-variable theory", *Mech. Adv. Mater. Struct.*, **24**(12), 987-998.

Barretta, R., Feo, L., Luciano, R. and de Sciarra, F.M. (2016), "Application of an enhanced version of the Eringen differential model to nanotechnology", *Compos. Part B: Eng.*, **96**, 274-280.

Barretta, R., Diaco, M., Feo, L., Luciano, R., de Sciarra, F.M. and Penna, R. (2018a), "Stress-driven integral elastic theory for torsion of nano-beams", *Mechanics Research Communications*, **87**, 35-41.

Barretta, R., Čanađija, M., Luciano, R. and de Sciarra, F.M. (2018b), "Stress-driven modeling of nonlocal thermoelastic behavior of nanobeams", *Int. J. Eng. Sci.*, **126**, 53-67.

Challamel, N. and Wang, C. (2008), "The small length scale effect for a non-local cantilever beam: a paradox solved", *Nanotech.*, **19**(34), 345703.

Chen, D., Yang, J. and Kitipornchai, S. (2015), "Elastic buckling and static bending of shear deformable functionally graded porous beam", *Compos. Struct.*, **133**, 54-61.

Dai, H.-L., Rao, Y.-N. and Dai, T. (2016), "A review of recent researches on FGM cylindrical structures under coupled physical interactions, 2000–2015", *Compos. Struct.*, **152**, 199-225.

Ebrahimi, F. and Daman, M. (2017), "Dynamic characteristics of curved inhomogeneous nonlocal porous beams in thermal environment", *Struct. Eng. Mech., Int. J.*, **64**(1), 121-133.

Ebrahimi, F. and Barati, M.R. (2017), "Porosity-dependent vibration analysis of piezo-magnetically actuated heterogeneous nanobeams", *Mech. Syst. Signal Process.*, **93**, 445-459.

Eltaher, M., Emam, S.A. and Mahmoud, F. (2012), "Free vibration analysis of functionally graded size-dependent nanobeams", *Appl. Math. Computat.*, **218**(14), 7406-7420.

Eringen, A.C. (1983), "On differential equations of nonlocal elasticity and solutions of screw dislocation and surface waves", *J. Appl. Phys.*, **54**(9), 4703-4710.

Ghorbanpour Arani, A., Mosayyebi, M., Kolahdouzan, F., Kolahchi, R. and Jamali, M. (2017), "Refined zigzag theory for vibration analysis of viscoelastic functionally graded carbon nanotube reinforced composite microplates integrated with piezoelectric layers", *Proceedings of the Institution of Mechanical Engineers, Part G: Journal of Aerospace Engineering*, **231**(13), 2464-2478.

Gupta, A. and Talha, M. (2017), "Influence of Porosity on the Flexural and Free Vibration Responses of Functionally Graded Plates in Thermal Environment", *Int. J. Struct. Stabil. Dyn.*, 1850013.

Hu, Y.G., Liew, K.M., Wang, Q., He, X.Q. and Yakobson, B.I. (2008), “Nonlocal shell model for elastic wave propagation in single- and double-walled carbon nanotubes”, *J. Mech. Phys. Solids*, **56**(12), 3475-3485.

Karami, B. and Janghorban, M. (2016), “Effect of magnetic field on the wave propagation in nanoplates based on strain gradient theory with one parameter and two-variable refined plate theory”, *Modern Phys. Lett. B*, **30**(36), 1650421.

Karami, B., Janghorban, M. and Tounsi, A. (2017), “Effects of triaxial magnetic field on the anisotropic nanoplates”, *Steel Compos. Struct., Int. J.*, **25**(3), 361-374.

Karami, B., Janghorban, M., Shahsavari, D. and Tounsi, A. (2018a), “A size-dependent quasi-3D model for wave dispersion analysis of FG nanoplates”, *Steel Compos. Struct., Int. J.*, **28**(1), 99-110.

Karami, B., Shahsavari, D., Karami, M. and Li, L. (2018b), “Hygrothermal wave characteristic of nanobeam-type inhomogeneous materials with porosity under magnetic field”, *Proceedings of the Institution of Mechanical Engineers, Part C: Journal of Mechanical Engineering Science*, 0954406218781680.

Karami, B., Shahsavari, D. and Li, L. (2018c), “Hygrothermal wave propagation in viscoelastic graphene under in-plane magnetic field based on nonlocal strain gradient theory”, *Physica E: Low-dimensional Syst. Nanostruct.*, **97**, 317-327.

Karami, B., Janghorban, M. and Tounsi, A. (2018d), “Nonlocal strain gradient 3D elasticity theory for anisotropic spherical nanoparticles”, *Steel Compos. Struct., Int. J.*, **27**(2), 201-216.

Karami, B., Janghorban, M. and Li, L. (2018e), “On guided wave propagation in fully clamped porous functionally graded nanoplates”, *Acta Astronautica*, **143**, 380-390.

Karami, B., Shahsavari, D. and Li, L. (2018f), “Temperature-dependent flexural wave propagation in nanoplate-type porous heterogenous material subjected to in-plane magnetic field”, *J. Therm. Stress.*, **41**(4), 483-499.

Karami, B., Shahsavari, D., Li, L., Karami, M. and Janghorban, M. (2018g), “Thermal buckling of embedded sandwich piezoelectric nanoplates with functionally graded core by a nonlocal second-order shear deformation theory”, *Proceedings of the Institution of Mechanical Engineers, Part C: Journal of Mechanical Engineering Science*.

Karami, B., Janghorban, M. and Tounsi, A. (2018h), “Variational approach for wave dispersion in anisotropic doubly-curved nanoshells based on a new nonlocal strain gradient higher order shell theory”, *Thin-Wall. Struct.*, **129**, 251-264.

Karami, B., Shahsavari, D., Janghorban, M. and Li, L. (2018i), “Wave dispersion of mounted graphene with initial stress”, *Thin-Wall. Struct.*, **122**, 102-111.

Karami, B., Shahsavari, D. and Janghorban, M. (2018j), “Wave propagation analysis in functionally graded (FG) nanoplates under in-plane magnetic field based on nonlocal strain gradient theory and four variable refined plate theory”, *Mech. Adv. Mater. Struct.*, **25**(12), 1047-1057.

Khdeir, A. and Reddy, J. (1999), “Free vibrations of laminated composite plates using second-order shear deformation theory”, *Comput. Struct.*, **71**(6), 617-626.

Khetir, H., Bouiadjra, M.B., Houari, M.S.A., Tounsi, A. and Mahmoud, S. (2017), “A new nonlocal trigonometric shear deformation theory for thermal buckling analysis of embedded nanosize FG plates”, *Struct. Eng. Mech., Int. J.*, **64**(4), 391-402.

Kneifati, M.C. (1985), “Analysis of plates on a Kerr foundation model”, *J. Eng. Mech.*, **111**(11), 1325-1342.

Kolahchi, R., Safari, M. and Esmailpour, M. (2016), “Dynamic stability analysis of temperature-dependent functionally graded CNT-reinforced visco-plates resting on orthotropic elastomeric medium”, *Compos. Struct.*, **150**, 255-265.

Li, L. and Hu, Y. (2017a), “Post-buckling analysis of functionally graded nanobeams incorporating nonlocal stress and microstructure-dependent strain gradient effects”, *Int. J. Mech. Sci.*, **120**, 159-170.

Li, L. and Hu, Y. (2017b), “Torsional vibration of bi-directional functionally graded nanotubes based on nonlocal elasticity theory”, *Compos. Struct.*, **172**, 242-250.

Li, J.F., Takagi, K., Ono, M., Pan, W., Watanabe, R., Almajid, A. and Taya, M. (2003), “Fabrication and evaluation of porous piezoelectric ceramics and porosity–graded piezoelectric actuators”, *J. Am. Ceramic Soc.*, **86**(7), 1094-1098.

Li, C., Yao, L., Chen, W. and Li, S. (2015), “Comments on nonlocal effects in nano-cantilever beams”, *Int. J. Eng. Sci.*, **87**, 47-57.

Li, L., Tang, H. and Hu, Y. (2018), “Size-dependent nonlinear vibration of beam-type porous materials with an initial geometrical curvature”, *Compos. Struct.*, **184**, 1177-1188.

Lim, C.W., Li, C. and Yu, J.-l. (2010), “Free vibration of pre-tensioned nanobeams based on nonlocal stress theory”, *J. Zhejiang Univ.-SCIENCE A*, **11**(1), 34-42.

Mechab, I., Mechab, B., Benaissa, S., Serier, B. and Bouiadjra, B. B. (2016a), “Free vibration analysis of FGM nanoplate with porosities resting on Winkler Pasternak elastic foundations based on two-variable refined plate theories”, *J. Brazil. Soc. Mech. Sci. Eng.*, **38**(8), 2193-2211.

Mechab, B., Mechab, I., Benaissa, S., Ameri, M. and Serier, B. (2016b), “Probabilistic analysis of effect of the porosities in functionally graded material nanoplate resting on Winkler–Pasternak elastic foundations”, *Appl. Math. Model.*, **40**(2), 738-749.

Mirzavand, B. and Eslami, M. (2011), “A closed-form solution for thermal buckling of piezoelectric FGM rectangular plates with temperature-dependent properties”, *Acta Mechanica*, **218**(1), 87-101.

Murmu, T. and Adhikari, S. (2012), “Nonlocal frequency analysis of nanoscale biosensors”, *Sensors and Actuators A: Physical*, **173**(1), 41-48.

Nami, M.R., Janghorban, M. and Damadam, M. (2015), “Thermal buckling analysis of functionally graded rectangular nanoplates based on nonlocal third-order shear deformation theory”, *Aerosp. Sci. Technol.*, **41**, 7-15.

Peddieson, J., Buchanan, G.R. and McNitt, R.P. (2003), “Application of nonlocal continuum models to nanotechnology”, *Int. J. Eng. Sci.*, **41**(3), 305-312.

Pradhan, S. and Murmu, T. (2010), “Application of nonlocal elasticity and DQM in the flapwise bending vibration of a rotating nanocantilever”, *Physica E: Low-dimensional Syst. Nanostruct.*, **42**(7), 1944-1949.

Pradhan, S. and Kumar, A. (2011), “Vibration analysis of orthotropic graphene sheets using nonlocal elasticity theory and differential quadrature method”, *Compos. Struct.*, **93**(2), 774-779.

Rad, A.B. and Shariyat, M. (2015), “Three-dimensional magneto-elastic analysis of asymmetric variable thickness porous FGM circular plates with non-uniform tractions and Kerr elastic foundations”, *Compos. Struct.*, **125**, 558-574.

Romano, G. and Barretta, R. (2017), “Nonlocal elasticity in nanobeams: the stress-driven integral model”, *Int. J. Eng. Sci.*, **115**, 14-27.

Romano, G., Barretta, R., Diaco, M. and de Sciarra, F.M. (2017a), “Constitutive boundary conditions and paradoxes in nonlocal elastic nanobeams”, *Int. J. Mech. Sci.*, **121**, 151-156.

Romano, G., Barretta, R. and Diaco, M. (2017b), “On nonlocal integral models for elastic nano-beams”, *Int. J. Mech. Sci.*, **131**, 490-499.

Romano, G., Luciano, R., Barretta, R. and Diaco, M. (2018), “Nonlocal integral elasticity in nanostructures, mixtures, boundary effects and limit behaviours", *Continuum Mech. Thermodyn.*, **30**, 641-655.

Rouzegar, J. and Abad, F. (2015), "Free vibration analysis of FG plate with piezoelectric layers using four-variable refined plate theory", *Thin-Wall. Struct.*, **89**, 76-83.

Shafiei, N. and Kazemi, M. (2017), "Nonlinear buckling of functionally graded nano-/micro-scaled porous beams", *Compos. Struct.*, **178**, 483-492.

Shafiei, N., Mousavi, A. and Ghadiri, M. (2016), "On size-dependent nonlinear vibration of porous and imperfect functionally graded tapered microbeams", *Int. J. Eng. Sci.*, **106**, 42-56.

Shahsavari, D. and Janghorban, M. (2017), "Bending and shearing responses for dynamic analysis of single-layer graphene sheets under moving load", *J. Brazil. Soc. Mech. Sci. Eng.*, **39**(10), 3849-3861.

Shahsavari, D., Shahsavari, M., Li, L. and Karami, B. (2017a), "A novel quasi-3D hyperbolic theory for free vibration of FG plates with porosities resting on Winkler/Pasternak/Kerr foundation", *Aerosp. Sci. Technol.*

Shahsavari, D., Karami, B., Janghorban, M. and Li, L. (2017b), "Dynamic characteristics of viscoelastic nanoplates under moving load embedded within visco-Pasternak substrate and hygrothermal environment", *Mater. Res. Express*, **4**(8), 085013.

Shahsavari, D., Karami, B., Fahham, H.R. and Li, L. (2018a), "On the shear buckling of porous nanoplates using a new size-dependent quasi-3D shear deformation theory", *Acta Mechanica*, 1-25.

Shahsavari, D., Karami, B. and Mansouri, S. (2018b), "Shear buckling of single layer graphene sheets in hygrothermal environment resting on elastic foundation based on different nonlocal strain gradient theories", *Eur. J. Mech.-A/Solids*, **67**, 200-214.

She, G.-L., Yuan, F.-G. and Ren, Y.-R. (2017a), "Nonlinear analysis of bending, thermal buckling and post-buckling for functionally graded tubes by using a refined beam theory", *Compos. Struct.*, **165**, 74-82.

She, G.-L., Yuan, F.-G. and Ren, Y.-R. (2017b), "Thermal buckling and post-buckling analysis of functionally graded beams based on a general higher-order shear deformation theory", *Appl. Math. Model.*, **47**, 340-357.

She, G.-L., Yuan, F.-G., Ren, Y.-R. and Xiao, W.-S. (2017c), "On buckling and postbuckling behavior of nanotubes", *Int. J. Eng. Sci.*, **121**, 130-142.

She, G.-L., Yuan, F.-G., Ren, Y.-R., Liu, H.-B. and Xiao, W.-S. (2018a), "Nonlinear bending and vibration analysis of functionally graded porous tubes via a nonlocal strain gradient theory", *Compos. Struct.*, **203**, 614-623.

She, G.-L., Ren, Y.-R., Yuan, F.-G. and Xiao, W.-S. (2018b), "On vibrations of porous nanotubes", *Int. J. Eng. Sci.*, **125**, 23-35.

She, G.-L., Yuan, F.-G. and Ren, Y.-R. (2018c), "On wave propagation of porous nanotubes", *Int. J. Eng. Sci.*, **130**, 62-74.

She, G.-L., Ren, Y.-R., Xiao, W.-S. and Liu, H. (2018d), "Study on thermal buckling and post-buckling behaviors of FGM tubes resting on elastic foundations", *Struct. Eng. Mech., Int. J.*, **66**(6), 729-736.

She, G.-L., Yan, K.-M., Zhang, Y.-L., Liu, H.-B. and Ren, Y.-R. (2018e), "Wave propagation of functionally graded porous nanobeams based on nonlocal strain gradient theory", *Eur. Phys. J. Plus*, **133**(9), 368.

Sobhy, M. (2017), "Hygro-thermo-mechanical vibration and buckling of exponentially graded nanoplates resting on elastic foundations via nonlocal elasticity theory", *Struct. Eng. Mech., Int. J.*, **63**(3), 401-415.

Touloukian, Y. and Buyco, E. (1970), *Thermophysical Properties of Matter*, The TPRC Data Series, Specific Heat of Metallic Elements and Alloys, (Volume 4), and Specific Heat of Nonmetallic Solids, (Volume 5), IFI: Plenum, New York, NY, USA.

Tounsi, A., Houari, M.S.A. and Benyoucef, S. (2013), "A refined trigonometric shear deformation theory for thermoelastic bending of functionally graded sandwich plates", *Aerosp. Sci. Technol.*, **24**(1), 209-220.

Wang, C. and Duan, W. (2008), "Free vibration of nanorings/arches based on nonlocal elasticity", *J. Appl. Phys.*, **104**(1), 014303.

Wang, L. and Hu, H. (2008), "Flexural Wave Propagation in Single-Walled Carbon Nanotubes", *J. Computat. Theor. Nanosci.*, **5**(4), 581-586.

Wang, Q. and Wang, C.M. (2007), "The constitutive relation and small scale parameter of nonlocal continuum mechanics for modelling carbon nanotubes", *Nanotechnology*, **18**(7), 075702.

Wattanasakulpong, N. and Ungbhakorn, V. (2014), "Linear and nonlinear vibration analysis of elastically restrained ends FGM beams with porosities", *Aerosp. Sci. Technol.*, **32**(1), 111-120.

Yahia, S.A., Atmane, H.A., Houari, M.S.A. and Tounsi, A. (2015), "Wave propagation in functionally graded plates with porosities using various higher-order shear deformation plate theories", *Struct. Eng. Mech., Int. J.*, **53**(6), 1143-1165.

Yang, H. and Yu, L. (2017), "Feature extraction of wood-hole defects using wavelet-based ultrasonic testing", *J. Forest. Res.*, **28**(2), 395-402.

Yang, J., Ke, L. and Kitipornchai, S. (2010), "Nonlinear free vibration of single-walled carbon nanotubes using nonlocal Timoshenko beam theory", *Physica E: Low-dimensional Syst. Nanostruct.*, **42**(5), 1727-1735.

Zhu, X. and Li, L. (2017a), "Closed form solution for a nonlocal strain gradient rod in tension", *Int. J. Eng. Sci.*, **119**, 16-28.

Zhu, X. and Li, L. (2017b), "Twisting statics of functionally graded nanotubes using Eringen's nonlocal integral model", *Compos. Struct.*, **178**, 87-96.

Zhu, J., Lai, Z., Yin, Z., Jeon, J. and Lee, S. (2001), "Fabrication of ZrO 2–NiCr functionally graded material by powder metallurgy", *Mater. Chem. Phys.*, **68**(1), 130-135.

CC